Supporting Information

Flexible Ligand and Halogen Engineering Enable One Phosphor-based Full-color Persistent Luminescence in Hybrid Perovskitoids

Guowei Xiao,†[a] Yu-Juan Ma,†[a] Zhenhong Qi,[a] Xiaoyu Fang,[a] Tianhong Chen [a] and Dongpeng Yan *[a]

[a] Beijing Key Laboratory of Energy Conversion and Storage Materials and Key Laboratory of Radiopharmaceuticals, Ministry of Education, College of Chemistry, Beijing Normal University, Beijing 100875, P. R. China

E-mail: yandp@bnu.edu.cn

† These authors contributed equally to this work.

Contents

Experimental Section

Experimental Section

Materials and methods

All chemicals were purchased from Beijing Innochem Science&Technology Co. Ltd. and used directly (analytical grade). All photoluminescence (PL) spectra and decay profiles were recorded on an FLS 980 fluorescence spectrometer, and the temperature-dependent PL spectra and decay curves were exported during the heating process. The UV lamp used to take photos for fluorescence and afterglow photos is 2 W. IR spectra were exported on a Shimadzu IRAffinity-1 FT-IR spectrometer using KBr pellet. Thermogravimetric analysis was carried out using a powder sample with a heating rate of 10 °C K^{-1} under N_2 atmosphere on a NETZSCH STA449 F5 synchronous thermal analyzer. The differential scanning calorimetry data were tested with a Mettler differential scanning calorimetry. The absorption spectra were measured on a Puxi Tu-1901 spectrophotometer using $BaSO_4$ as reference. Powder X-ray diffraction (PXRD) data were recorded on a Shimadzu XRD-7000 (3KW) X-ray diffractometer. Simulated curves of PXRD were exported by diffraction-crystal module of the Mercury (Hg) program using the single-crystal data.

Synthetic procedures

Synthesis of CdCl-apim1. 0.20 mmol $CdCl_2{\cdot}2.5H_2O$ (0.045 g), 0.40 mmol apim (0.065 mL), 1 mL deionized water, 3 mL ethanol and 0.2 mL concentrated hydrochloric acid were sealed in a Teflon-lined autoclave (20 mL) and heated to 120 °C for 72 hours. Colorless crystals were obtained and washed with absolute ethanol. Yield: ca. 52% based on $CdCl_2{\cdot}2.5H_2O$.

Synthesis of CdBr-apim1. 0.20 mmol $CdBr_2{\cdot}4H_2O$ (0.069 g), 0.40 mmol apim (0.065 mL), 1 mL deionized water, 3 mL EtOH and 0.2 mL concentrated hydrobromic acid were added in a glass bottle (15 mL), then dissolved by ultrasound and evaporated for several days. Colorless crystals were obtained. Yield: *ca.* 26% based on $CdBr_2{\cdot}4H_2O$.

Synthesis of CdCl-apim2. 0.20 mmol $CdCl_2{\cdot}2.5H_2O$ (0.045 g), 0.80 mmol apim (0.13 mL), 3 mL deionized water, 6 mL acetonitrile and 0.15 mL concentrated hydrochloric acid were sealed in a Teflon-lined autoclave (20 mL) and heated to 120 °C for 72 hours. Colorless crystals were obtained and washed with absolute ethanol. Yield: *ca.* 38% based on $CdCl_2{\cdot}2.5H_2O$.

Synthesis of CdBr-apim2. 0.20 mmol $CdBr_2{\cdot}4H_2O$ (0.103 g), 0.60 mmol apim (0.095 mL), 5 mL deionized water and 0.05 mL concentrated hydrobromic acid were sealed in a Teflon-lined autoclave (20 mL) and heated to 140 °C for 72 hours. Colorless crystals were obtained and washed with absolute ethanol. Yield: *ca.* 34% based on $CdBr_2{\cdot}4H_2O$.

Preparation of Ink. CdBr-apim2 is carefully ground and sieved through a 200 mesh screen, and poly(methylmethacrylate) (PMMA) is dissolved in moderate acetonitrile. Then the sieved powders can be mixed with a concentration of **CdBr-apim2** at 10%.

Crystallography.

The single-crystal X-ray diffraction data were collected on a Rigaku XtalLAB Synergy diffractometer with Cu-Kα radiation (λ = 1.54184 Å). SHELX-2016 software was employed to solve and refine the structure.[1] Crystallographic data are listed in Table S1 and S3, while selected bond lengths and angles are listed in Table S2, S4 and S5. Full crystallographic data for perovskitoids has been deposited with the CCDC (2253383-2253388).

Calculation Details

The density functional theory (DFT) and the time-dependent density functional theory (TDDFT) are performed via CP2K 9.1[2] to optimize the geometries of ground state and excited triplet states of 1D structure and 2D structure using the PBE functional using the DZVP-MOLOPT-SR-GTH basis set for all elements. The D3 Grimme's dispersion term with Becke-Johnson damping is added to the PBE functional to better describe the intramolecular non-covalent interactions between the metal-organic complexes. k-point is set by GAMMA only. The input files are generated by Multiwfn[3-5]. Based on calculation result, charge density difference is calculated by Multiwfn and graphs are analyzed by VESTA[6].

References

1 G. M. Sheldrick, *Acta Crystallogr. C*, 2015, **71**, 3−8.
2 T. D. Kühne, M. Iannuzzi, M. Del Ben, V. V. Rybkin, P. Seewald, F. Stein, T. Laino, R. Z. Khaliullin, O. Schütt, F. Schiffmann, D. Golze, J. Wilhelm, S. Chulkov, M. H. Bani-Hashemian, V. Weber, U. Borštnik, M. Taillefumier, A. S. Jakobovits, A. Lazzaro, H. Pabst, T. Müller, R. Schade, M. Guidon, S. Andermatt, N. Holmberg, G. K. Schenter, A. Hehn, A. Bussy, F. Belleflamme, G. Tabacchi, A. Glöß, M. Lass, I. Bethune, C. J. Mundy, C. Plessl, M. Watkins, J. VandeVondele, M. Krack and J. Hutter, *J. Chem. Phys.*, 2020, **152**, 194103.
3 T. Lu and F. Chen, *J. Comput. Chem.*, 2012, **33**, 580−592.
4 T. Lu and Q. Chen, *J. Comput. Chem.*, 2022, **43**, 539−555.
5 T. Lu and Q. Chen, ChemRxiv. Cambridge: Cambridge Open Engage, 2020.
6 K. Momma and F. Izumi, *J. Appl. Crystallogr.*, 2011, **44**, 1272−1276.

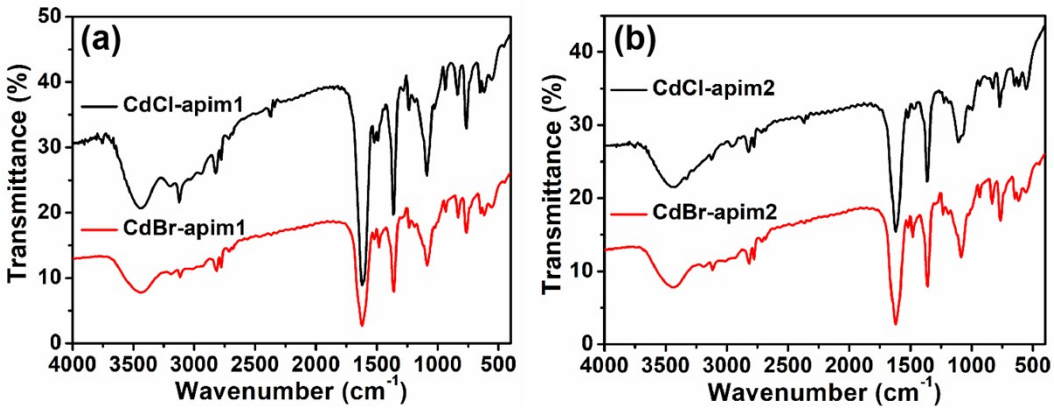

Figure S1. IR plots of (a) **CdX-apim1** and (b) **CdX-apim2** (X = Cl, Br).

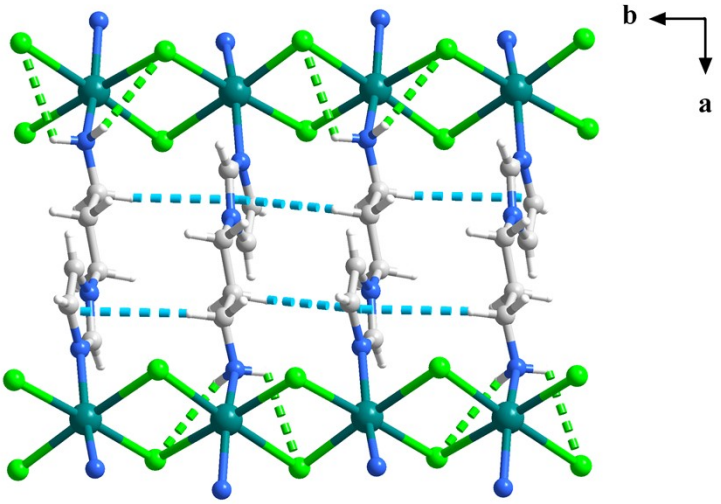

Figure S2. The structure of **CdCl-apim2** along *c* axis, in which green and blue dashed represent N-H...Cl and C-H...π interactions, respectively.

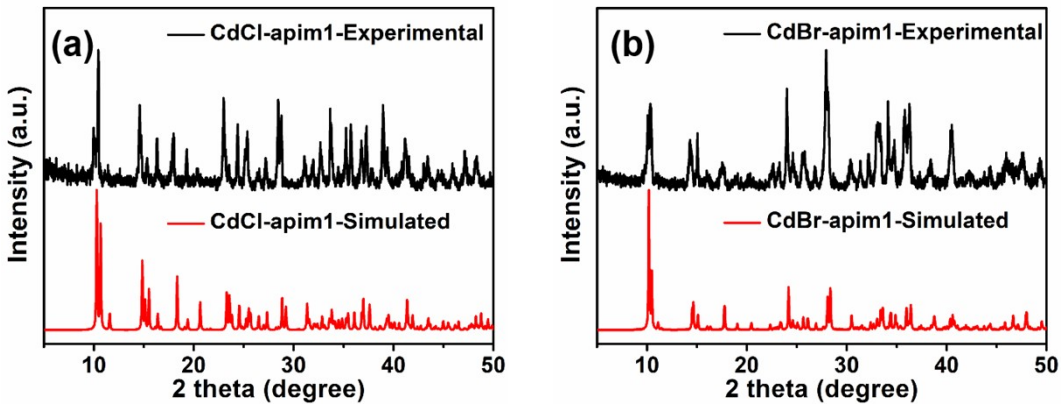

Figure S3. The PXRD plots for **CdCl-apim1** (a) and **CdBr-apim1** (b).

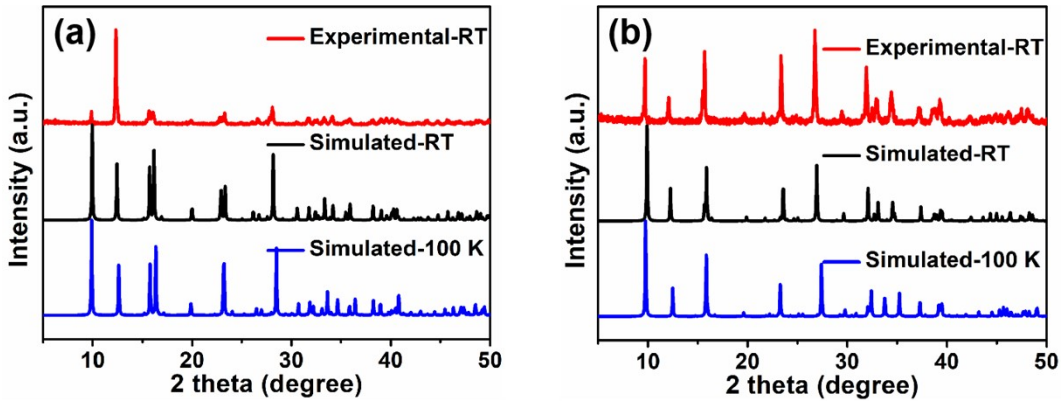

Figure S4. The PXRD plots for **CdCl-apim2** (a) and **CdBr-apim2** (b).

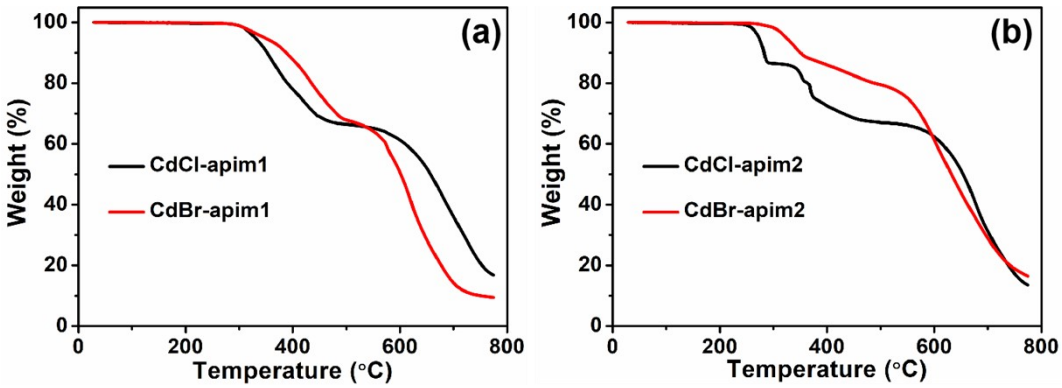

Figure S5. TGA plots of (a) **CdX-apim1** and (b) **CdX-apim2** (X = Cl, Br).

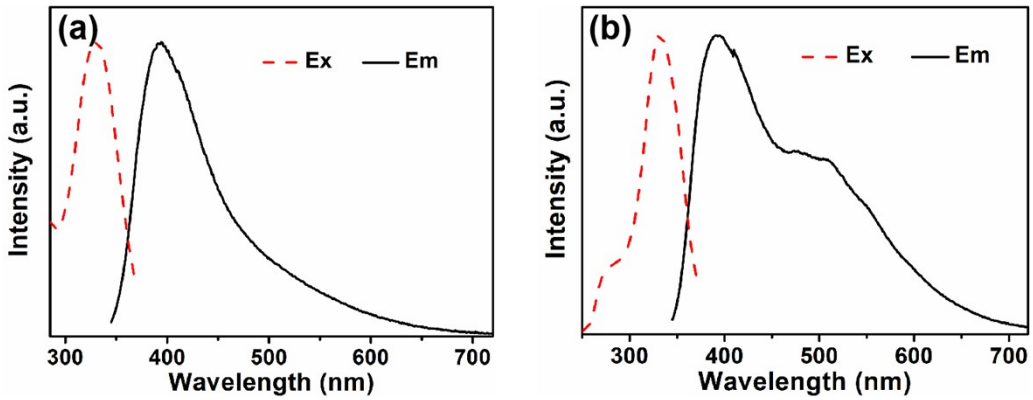

Figure S6. The excitation and emission spectra of **CdCl-apim1** (a) and **CdBr-apim1** (b).

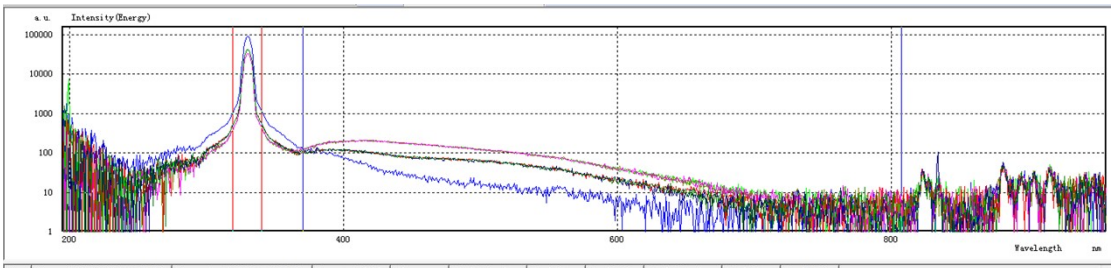

N ...	Cursor1-2: 319.23 - 340.47(...	Cursor3-4: 370.77 - 807.45(...	QuantumYield	Abs	Peak Wavele...	Peak Co...	Peak FW...	Peak Wavele...	Peak Co...	Peak FW...
1	183795686	---	---	---	329.86	88348.27	5.99	380.61	140.33	129.56
2	68327482	13156885	0.114	0.628	329.86	32845.41	5.98	411.58	210.09	153.37
3	68415189	13043888	0.113	0.628	329.86	32902.44	5.99	416.11	210.43	148.38
4	68382419	13101810	0.114	0.628	329.86	32935.46	5.98	415.35	211.77	155.13
5	86956051	6064195	0.063	0.527	329.86	41484.29	6.03	380.61	130.36	183.37
6	86875592	5925715	0.061	0.527	329.86	41431.35	6.03	389.68	129.02	190.26
7	87014461	6040626	0.062	0.527	329.86	41542.41	6.03	388.92	128.10	200.61

Figure S7. Quantum yields of **CdX-apim1** under 330 nm UV light excitation (1 for background; 2-4 for **CdCl-apim1**; 5-7 for **CdBr-apim1**).

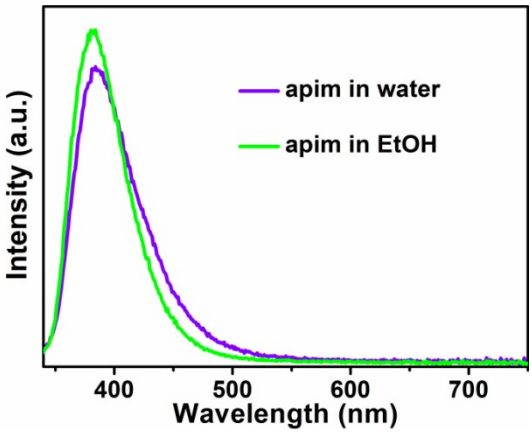

Figure S8. Prompt emission spectra of apim in water and EtOH solutions.

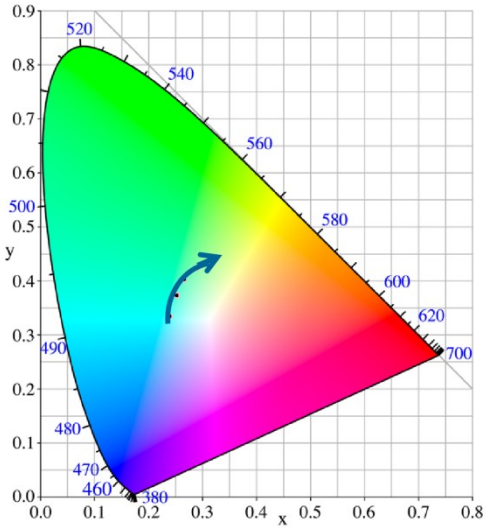

Figure S9. The excitation wavelength-dependent CIE coordinates in delayed mode for **CdCl-apim1**.

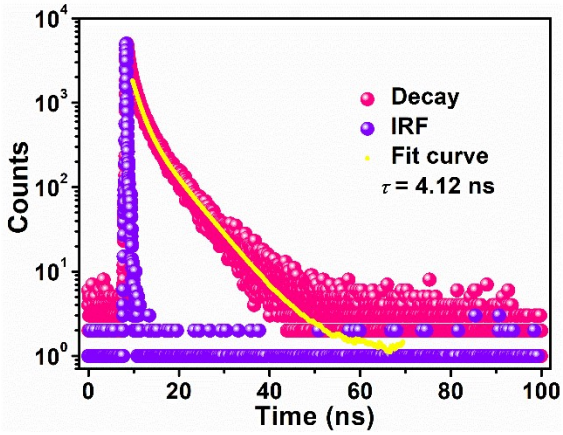

Figure S10. Fluorescence decay profile of **CdBr-apim1**.

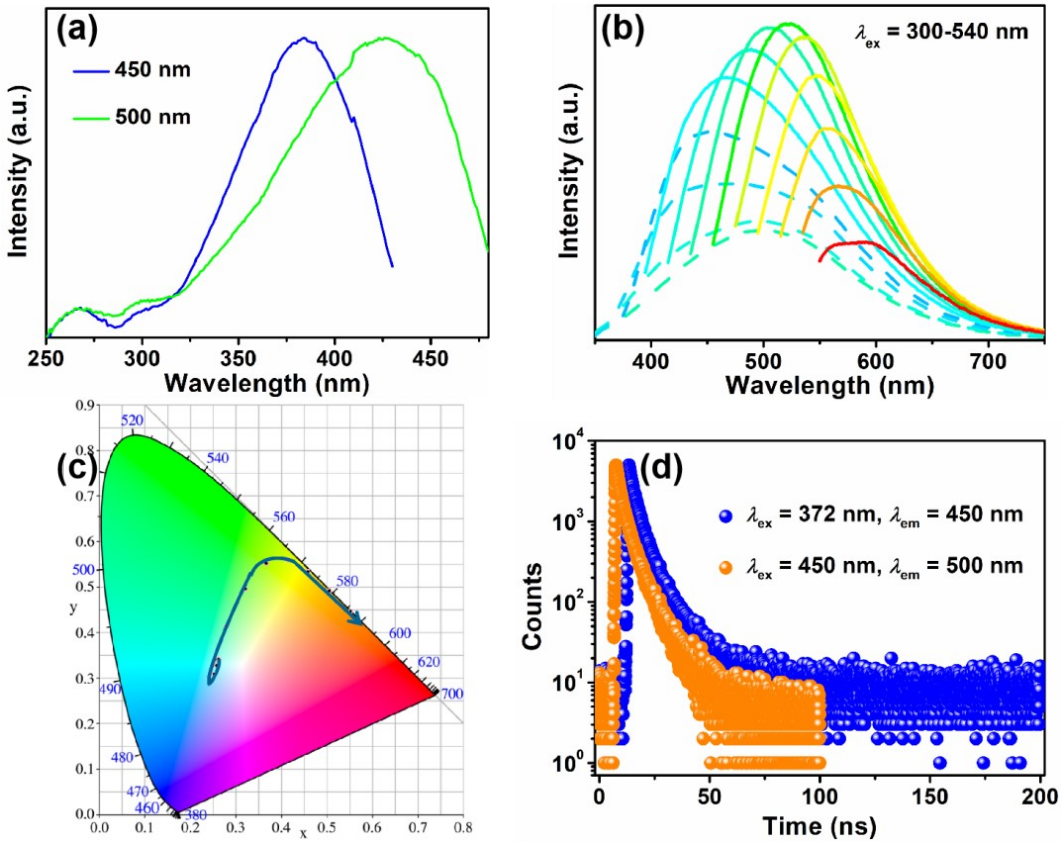

Figure S11. (a) Excitation spectra of **CdCl-apim2** monitored at 450 nm and 500 nm; (b,c) Prompt PL spectra and CIE coordinates of **CdCl-apim2** under different excitations; (d) Fluorescence decay profiles at 450 nm and 500 nm.

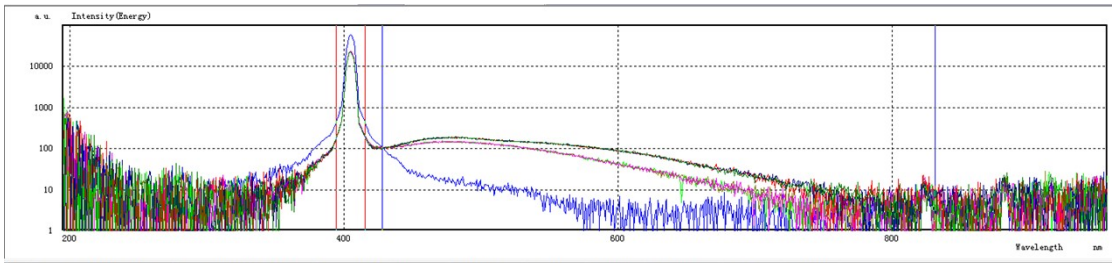

N ...	Cursor1-2: 394.21 - 415.35(...	Cursor3-4: 428.18 - 831.60(...	QuantumYield	Abs	Peak Wavele...	Peak Co...	Peak FW...	Peak Wavele...	Peak Co...	Peak FW...
1	139130147	---	---	---	404.79	57375.58	5.74	428.93	105.28	67.51
2	56066832	9858298	0.119	0.597	404.79	22992.17	5.76	477.10	152.04	166.83
3	56106559	9763938	0.118	0.597	404.79	23048.49	5.75	471.84	153.58	168.20
4	56097307	9772848	0.118	0.597	404.79	22994.58	5.77	480.86	150.64	168.92
5	53829581	15259425	0.179	0.613	404.79	21990.63	5.77	478.60	192.40	160.26
6	53871513	15225328	0.179	0.613	404.79	21996.18	5.77	481.61	190.84	201.28
7	53883309	15315104	0.180	0.613	404.79	22035.44	5.77	486.11	193.20	199.28

Figure S12. Quantum yields of **CdX-apim2** under 405 nm UV light excitation (1 for background; 2-4 for **CdCl-apim2**; 5-7 for **CdBr-apim2**).

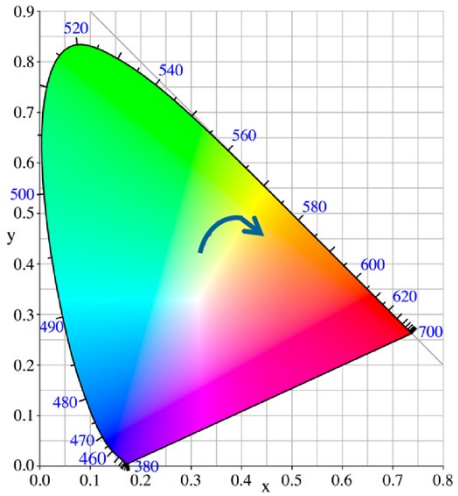

Figure S13. The excitation wavelength-dependent CIE coordinates in delayed mode for **CdCl-apim2**.

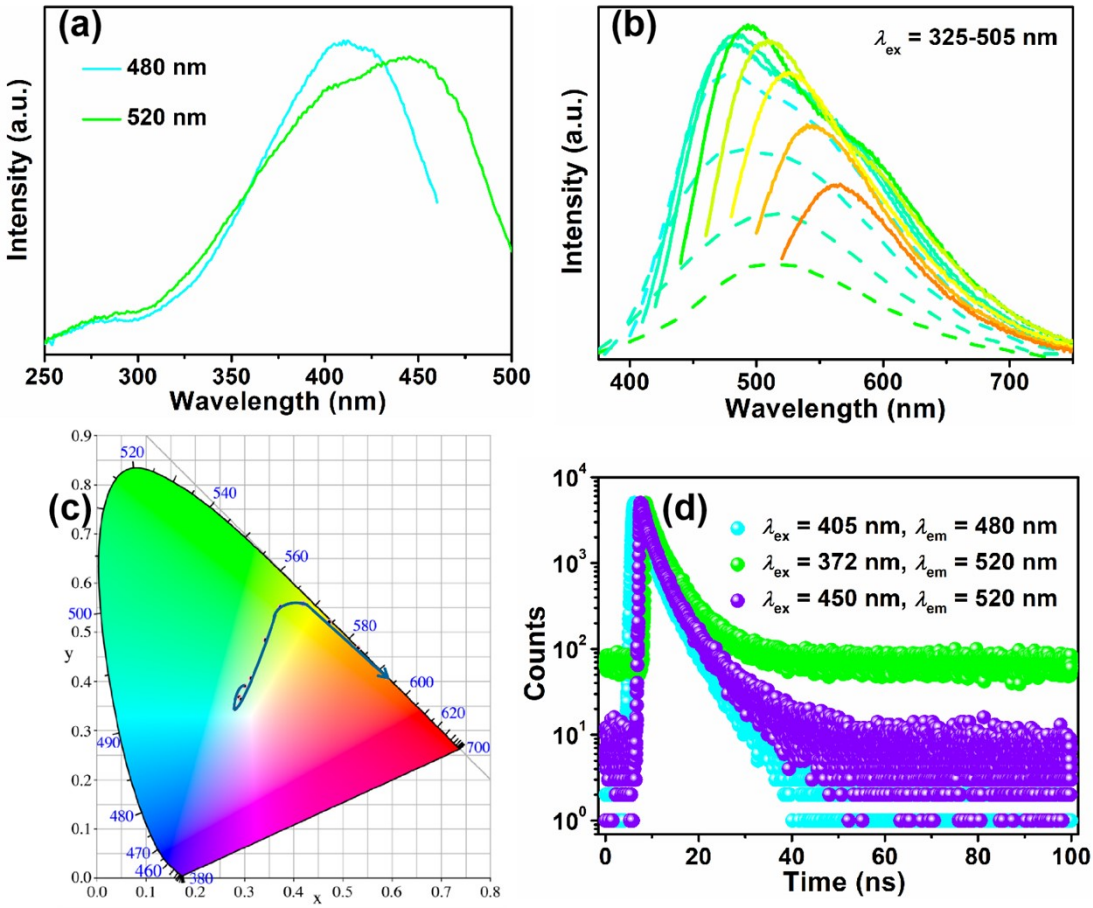

Figure S14. (a) Excitation spectra of **CdBr-apim2** monitored at 480 nm and 520 nm; (b, c) Prompt PL spectra and CIE coordinates of **CdBr-apim2** under different excitations; (d) Fluorescence decay profiles at 480 nm and 520 nm.

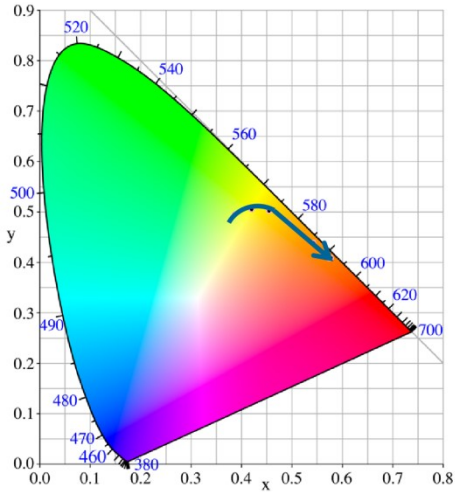

Figure S15. The excitation wavelength-dependent CIE coordinates in delayed mode for **CdBr-apim2**.

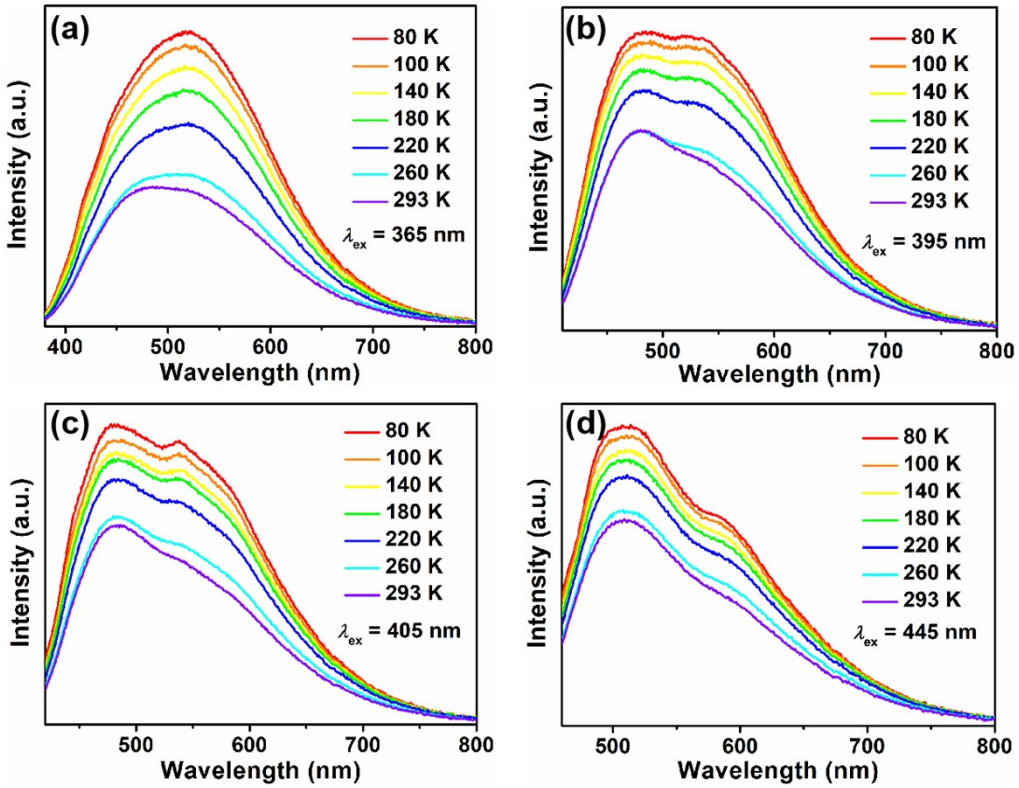

Figure S16 The temperature-dependent emission spectra for **CdBr-apim2** excited by different UV lights (Prompt mode).

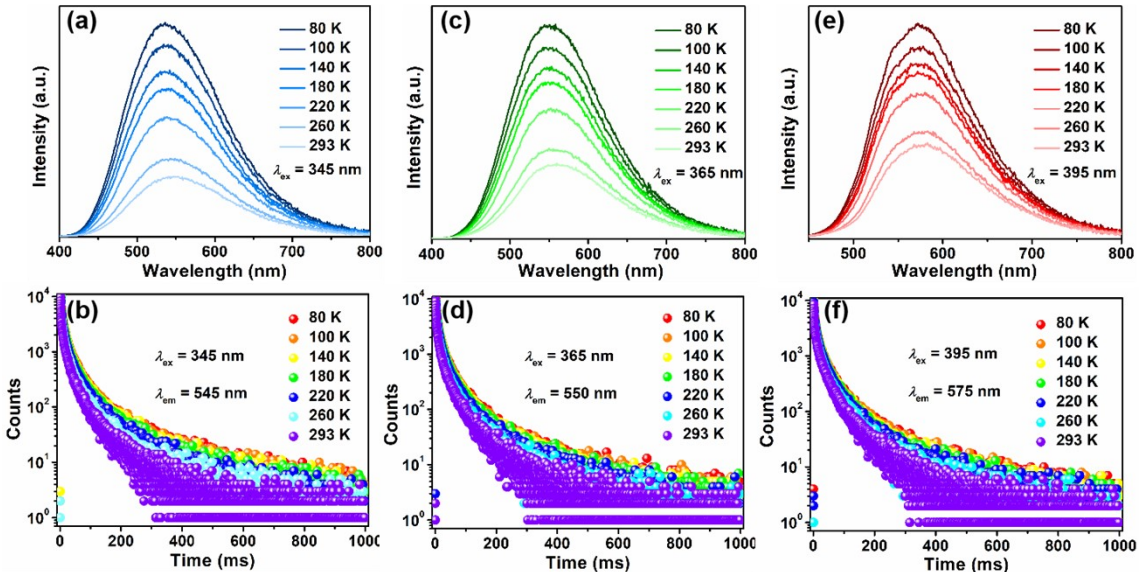

Figure S17. (a, c, e) The temperature-dependent emission spectra for **CdBr-apim2** excited by different UV lights (Delayed mode); (b, d, f) Decay profiles excited by different UV lights.

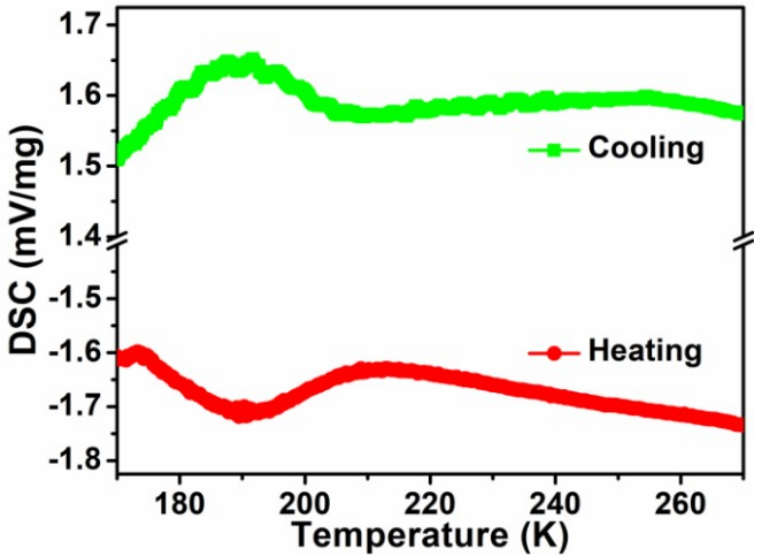

Figure S18. Differential scanning calorimetry (DSC) plots for **CdBr-apim2**.

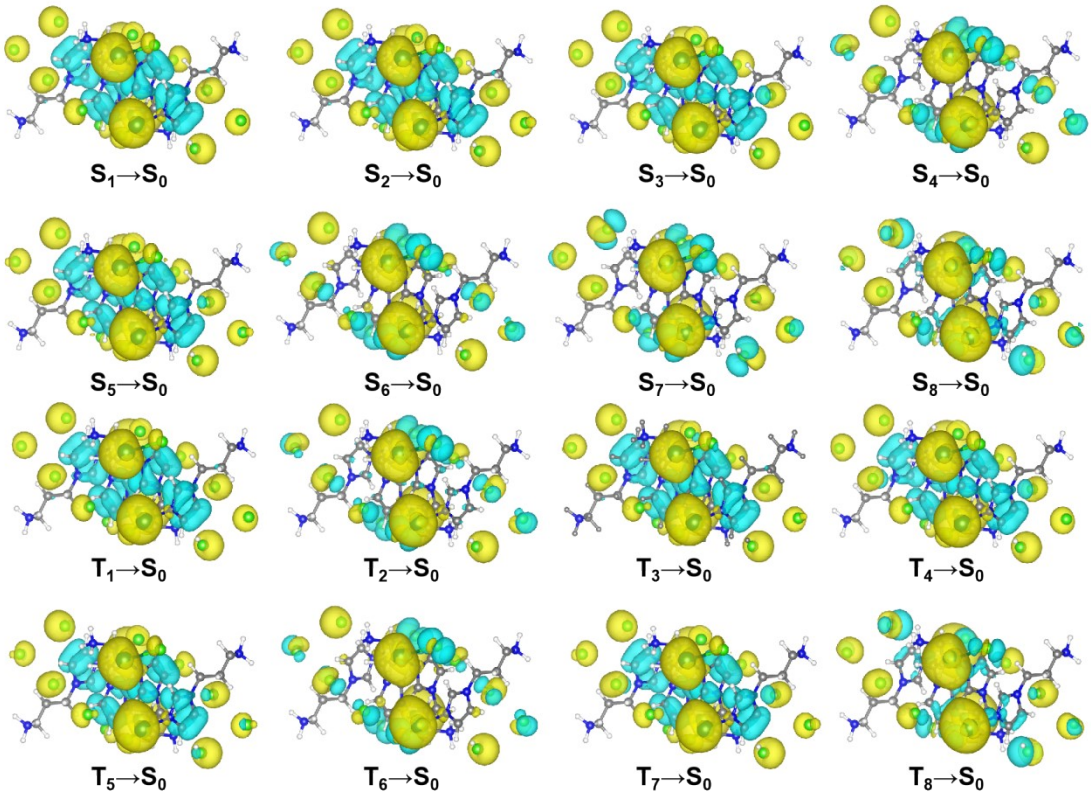

Figure S19. Distribution maps of the hole and electron in emission processes, for **CdCl-apim1** (Hole, yellow; Electron, cyan).

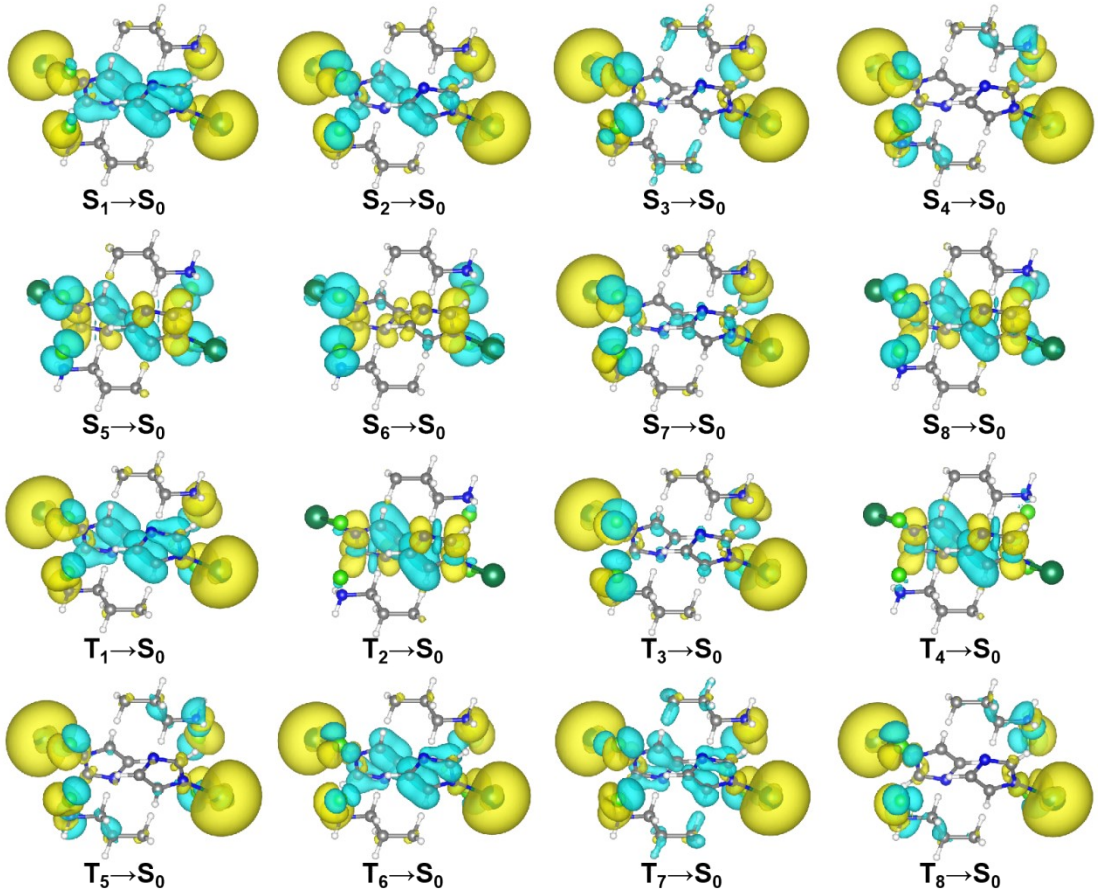

Figure S20. Distribution maps of the hole and electron in emission processes, for **CdCl-apim2** (Hole, yellow; Electron, cyan).

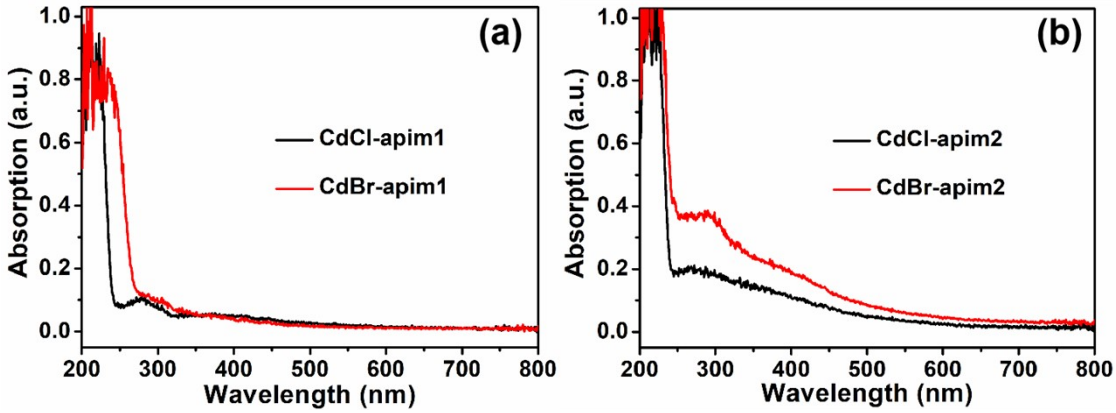

Figure S21. UV−vis absorption spectra of **CdX-apim1** and **CdX-apim2**.

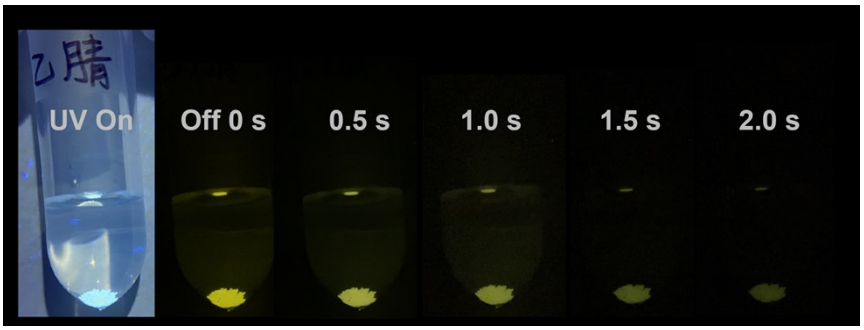

Figure S22. Images of **CdBr-apim2** immersed in acetonitrile before and after turning off the 365 nm UV lamp.

Table S1. Crystallographic data for **CdCl-apim1** and **CdBr-apim1**.

	CdCl-apim1	**CdBr-apim1**
Formula	$C_6H_{12}N_3CdCl_3$	$C_6H_{12}N_3CdBr_3$
*M*r (g·mol^{-1})	344.94	478.32
Temperature (K)	100 K	100 K
Space group	*P*2/c	*P*2/c
Crystal system	Monoclinic	Monoclinic
a (Å)	7.6542(2)	7.99480(10)
b (Å)	8.5911(3)	8.67360(10)
c (Å)	16.6247(5)	16.9504(3)
α (°)	90	90
β (°)	94.622(3)	95.696(2)
γ (°)	90	90
V (Å^3)	1089.65(6)	1169.60(3)
Z	4	4
F(000)	672	888
Dc (gcm^{-3})	2.103	2.716
μ (mm^{-1})	22.498	26.664
R_{int}	0.0450	0.0738
	-9≤h≤9	-10≤h≤7
limiting indices	-10≤k≤10	-10≤k≤10
	-20≤l≤16	-20≤l≤20
Collected reflections	12133	13387
Unique reflections	2249	2383
GOF on F^2	1.024	1.041
R_1, wR_2 [I>2σ(I)]	0.0494 0.1297	0.0540 0.1597
R_1, wR_2 [all data]	0.0497 0.1299	0.0550 0.1611

[a] $R_1 = \sum ||F_o| - |F_c|| / \sum |F_o|$. [b] $wR_2 = \{\sum[w(F_o^2 - F_c^2)^2] / \sum w(F_o^2)^2\}^{1/2}$.

Table S2. Selected bond lengths (Å) and angles (°) for **CdCl-apim1** and **CdBr-apim1** at 100 K.

CdCl-apim1		**CdBr-apim1**	
Cd(1)-N(1)	2.253(6)	Cd(1)-N(1)	2.253(6)
Cd(1)-Cl(3)	2.5674(16)	Cd(1)-Br(4)	2.6901(8)
Cd(1)-Cl(2)	2.6401(10)	Cd(1)-Br(3)	2.7881(6)
Cd(1)-Cl(1)	2.6947(16)	Cd(1)-Br(1)#1	2.8185(8)
Cd(1)-Cl(1)#1	2.7043(15)	Cd(1)-Br(1)	2.8387(8)
Cd(1)-Cl(4)	2.7157(17)	Cd(1)-Br(2)	2.8828(9)
N(1)-Cd(1)-Cl(3)	97.82(15)	N(1)-Cd(1)-Br(4)	99.05(15)
N(1)-Cd(1)-Cl(2)	97.45(15)	N(1)-Cd(1)-Br(3)	96.10(16)
Cl(3)-Cd(1)-Cl(2)	91.50(5)	Br(4)-Cd(1)-Br(3)	91.61(2)
N(1)-Cd(1)-Cl(1)	87.77(15)	N(1)-Cd(1)-Br(1)#1	87.25(16)
Cl(3)-Cd(1)-Cl(1)	171.94(5)	Br(4)-Cd(1)-Br(1)#1	92.60(2)
Cl(2)-Cd(1)-Cl(1)	93.54(4)	Br(3)-Cd(1)-Br(1)#1	174.15(2)
N(1)-Cd(1)-Cl(1)#1	86.10(15)	N(1)-Cd(1)-Br(1)	87.30(15)
Cl(3)-Cd(1)-Cl(1)#1	92.18(5)	Br(4)-Cd(1)-Br(1)	172.22(3)
Cl(2)-Cd(1)-Cl(1)#1	174.50(4)	Br(3)-Cd(1)-Br(1)	92.18(2)
Cl(1)-Cd(1)-Cl(1)#1	82.37(5)	Br(1)#1-Cd(1)-Br(1)	83.16(3)
N(1)-Cd(1)-Cl(4)	163.21(15)	N(1)-Cd(1)-Br(2)	164.96(15)
Cl(3)-Cd(1)-Cl(4)	92.68(5)	Br(4)-Cd(1)-Br(2)	91.63(2)
Cl(2)-Cd(1)-Cl(4)	95.33(5)	Br(3)-Cd(1)-Br(2)	94.15(2)
Cl(1)-Cd(1)-Cl(4)	80.59(4)	Br(1)#1-Cd(1)-Br(2)	81.67(2)
Cl(1)#1-Cd(1)-Cl(4)	80.42(4)	Br(1)-Cd(1)-Br(2)	81.32(2)
Symmetry codes: #1: -x, y, -z+1/2; #2: -x+1, y, -z+1/2.		Symmetry codes: #1: -x, y, -z+1/2; #2: -x+1, y, -z+1/2.	

Table S3. Crystallographic data for **CdCl-apim2** and **CdBr-apim2**.

	CdCl-apim2				**CdBr-apim2**			
Formula	$C_6H_{11}N_3CdC_{l2}$		$C_6H_{11}N_3CdCl_2$		$C_6H_{11}N_3CdBr_2$		$C_6H_{11}N_3CdBr_2$	
*M*r (g·mol^{-1})	308.48		308.48		397.40		397.40	
Temperature (K)	100 K		282 K		100 K		282 K	
Space group	$P2_1/c$		$P2_1/m$		$P2_1/c$		$P2_1/m$	
Crystal system	Monoclinic		Monoclinic		Monoclinic		Monoclinic	
a (Å)	8.9307(3)		7.1135(3)		9.0513(2)		7.2184(2)	
b (Å)	7.6716(2)		7.7569(3)		8.0055(2)		8.1651(2)	
c (Å)	14.0159(4)		8.8801(4)		14.1660(3)		8.9205(2)	
α (°)	90		90		90		90	
β (°)	92.145(3)		91.575(3)		90.092(2)		90.782(2)	
γ (°)	90		90		90		90	
V (Å^3)	959.60(5)		489.81(4)		1026.47(4)		525.72(2)	
Z	4		2		4		2	
F(000)	600		300		744		372	
Dc (gcm^{-3})	2.135		2.092		2.572		2.510	
μ (mm^{-1})	22.945		22.476		25.784		25.172	
R_{int}	0.0832		0.0551		0.0436		0.0400	
	-11≤h≤11		-9≤h≤8		-11≤h≤11		-8≤h≤7	
limiting indices	-9≤k≤9		-9≤k≤9		-9≤k≤10		-10≤k≤10	
	-17≤l≤17		-10≤l≤10		-15≤l≤17		-11≤l≤11	
Collected reflections	10184		4332		11210		5187	
Unique reflections	1955		1062		2100		1137	
GOF on F^2	1.052		1.042		1.048		1.028	
R_1, wR_2 [$I>2\sigma(I)$]	0.0600	0.1885	0.0641	0.1819	0.0524	0.1518	0.0494	0.1429
R_1, wR_2 [all data]	0.0616	0.1893	0.0664	0.1906	0.0533	0.1522	0.0502	0.1437

[a] $R_1 = \sum ||F_o| - |F_c|| / \sum |F_o|$. [b] $wR_2 = \{\sum [w(F_o^2 - F_c^2)^2] / \sum w(F_o^2)^2\}^{1/2}$.

Table S4. Continuous Shape Measure (CShM) analyses of geometries for Cd1 in compounds **CdCl-apim2** and **CdBr-apim2** by SHAPE 2.0 Software.

Geometry	**CdCl-apim2-100K**-Cd1	**CdCl-apim2-282K**-Cd1	**CdBr-apim2-100K**-Cd1	**CdBr-apim2-282K**-Cd1
Hexagon(D_{6h})	31.937	31.673	32.473	32.031
Pentagonal pyramid(C_{5v})	23.643	23.411	23.679	23.435
Octahedron(O_h)	1.179	1.309	1.627	1.891
Trigonal prism(D_{3h})	14.177	14.304	14.761	15.047
Johnson pentagonal pyramid J2(C_{5v})	26.547	26.216	26.160	25.779

Table S5. Selected bond lengths (Å) and angles (°) for **CdCl-apim2** at different temperatures.

100 K		**282 K**	
Cd(1)-N(1)	2.284(8)	Cd(1)-N(1)	2.272(8)
Cd(1)-N(3)#1	2.298(9)	Cd(1)-N(3)#1	2.298(10)
Cd(1)-Cl(1)	2.586(2)	Cd(1)-Cl(1)	2.5844(19)
Cd(1)-Cl(2)#2	2.601(2)	Cd(1)-Cl(1)#2	2.5844(19)
Cd(1)-Cl(2)	2.775(2)	Cd(1)-Cl(1)#3	2.829(2)
Cd(1)-Cl(1)#2	2.787(2)	Cd(1)-Cl(1)#4	2.829(2)
Cd(1)-Cd(1) intrachain	3.846	Cd(1)-Cd(1) intrachain	3.893
Cd(1)-Cd(1) interchain	11.560	Cd(1)-Cd(1) interchain	11.530
N(1)-Cd(1)-N(3)#1	159.6(3)	N(1)-Cd(1)-N(3)#1	158.0(4)
N(1)-Cd(1)-Cl(1)	98.8(2)	N(1)-Cd(1)-Cl(1)	97.99(17)
N(3)#1-Cd(1)-Cl(1)	97.1(2)	N(3)#1-Cd(1)-Cl(1)	97.00(17)
N(1)-Cd(1)-Cl(2)#2	96.6(2)	N(1)-Cd(1)-Cl(1)#2	97.99(17)
N(3)#1-Cd(1)-Cl(2)#2	95.3(2)	N(3)#1-Cd(1)-Cl(1)#2	97.00(18)
Cl(1)-Cd(1)-Cl(2)#2	92.91(7)	Cl(1)-Cd(1)-Cl(1)#2	93.90(8)
N(1)-Cd(1)-Cl(2)	87.7(2)	N(1)-Cd(1)-Cl(1)#3	86.60(18)

N(3)#1-Cd(1)-Cl(2)	79.9(2)	N(3)#1-Cd(1)-Cl(1)#3	77.83(18)
Cl(1)-Cd(1)-Cl(2)	88.52(7)	Cl(1)-Cd(1)-Cl(1)#3	88.14(6)
Cl(2)#2-Cd(1)-Cl(2)	175.22(4)	Cl(1)#2-Cd(1)-Cl(1)#3	174.66(3)
N(1)-Cd(1)-Cl(1)#2	85.9(2)	N(1)-Cd(1)-Cl(1)#4	86.60(18)
N(3)#1-Cd(1)-Cl(1)#2	77.9(2)	N(3)#1-Cd(1)-Cl(1)#4	77.83(18)
Cl(1)-Cd(1)-Cl(1)#2	175.05(3)	Cl(1)-Cd(1)-Cl(1)#4	174.66(3)
Cl(2)#2-Cd(1)-Cl(1)#2	87.97(7)	Cl(1)#2-Cd(1)-Cl(1)#4	88.13(6)
Cl(2)-Cd(1)-Cl(1)#2	90.22(7)	Cl(1)#3-Cd(1)-Cl(1)#4	89.42(8)
Symmetry codes: #1: x-1, -y+1/2, z+1/2; #2: -x, y+1/2, -z+3/2; #3: -x, y-1/2, -z+3/2; #4: x+1, -y+1/2, z-1/2.		Symmetry codes: #1: x+1, y, z-1; #2: x, -y+1/2, z; #3: -x+1, -y+1, -z; #4: -x+1, y-1/2, -z; #5: x-1, y, z+1.	

Table S6. Selected bond lengths (Å) and angles (°) for **CdBr-apim2** at different temperatures.

100 K		**282 K**	
Cd(1)-N(1)	2.268(7)	Cd(1)-N(1)	2.258(7)
Cd(1)-N(3)#1	2.272(8)	Cd(1)-N(3)#1	2.261(10)
Cd(1)-Br(1)	2.7137(10)	Cd(1)-Br(1)#2	2.7146(9)
Cd(1)-Br(2)#2	2.7364(10)	Cd(1)-Br(1)#3	2.7146(9)
Cd(1)-Br(2)	2.9159(10)	Cd(1)-Br(1)#4	3.0229(9)
Cd(1)-Br(1)#2	2.9494(10)	Cd(1)-Br(1)	3.0230(9)
Cd(1)-Cd(1) intrachain	4.102	Cd(1)-Cd(1) intrachain	4.101
Cd(1)-Cd(1) interchain	11.507	Cd(1)-Cd(1) interchain	11.398
N(1)-Cd(1)-N(3)#1	159.1(3)	N(1)-Cd(1)-N(3)#1	156.7(3)
N(1)-Cd(1)-Br(1)	98.9(2)	N(1)-Cd(1)-Br(1)#2	98.03(13)
N(3)#1-Cd(1)-Br(1)	98.3(2)	N(3)#1-Cd(1)-Br(1)#2	97.84(18)
N(1)-Cd(1)-Br(2)#2	96.09(19)	N(1)-Cd(1)-Br(1)#3	98.03(13)
N(3)#1-Cd(1)-Br(2)#2	95.2(2)	N(3)#1-Cd(1)-Br(1)#3	97.84(17)

Br(1)-Cd(1)-Br(2)#2	91.59(3)	Br(1)#2-Cd(1)-Br(1)#3	93.59(4)
N(1)-Cd(1)-Br(2)	87.53(19)	N(1)-Cd(1)-Br(1)#4	86.12(14)
N(3)#1-Cd(1)-Br(2)	80.7(2)	N(3)#1-Cd(1)-Br(1)#4	77.28(18)
Br(1)-Cd(1)-Br(2)	89.88(3)	Br(1)#2-Cd(1)-Br(1)#4	174.79(2)
Br(2)#2-Cd(1)-Br(2)	175.84(3)	Br(1)#3-Cd(1)-Br(1)#4	88.93(2)
N(1)-Cd(1)-Br(1)#2	85.3(2)	N(1)-Cd(1)-Br(1)	86.12(14)
N(3)#1-Cd(1)-Br(1)#2	77.5(2)	N(3)#1-Cd(1)-Br(1)	77.28(18)
Br(1)-Cd(1)-Br(1)#2	175.75(2)	Br(1)#2-Cd(1)-Br(1)	88.93(2)
Br(2)#2-Cd(1)-Br(1)#2	88.74(3)	Br(1)#3-Cd(1)-Br(1)	174.79(2)
Br(2)-Cd(1)-Br(1)#2	89.50(3)	Br(1)#4-Cd(1)-Br(1)	88.21(3)

Symmetry codes: #1: x-1, -y+1/2, z+1/2; #2: -x, y-1/2, -z+1/2; #3: -x, y+1/2, -z+1/2; #4: x+1, -y+1/2, z-1/2.

Symmetry codes: #1: x+1, y, z+1; #2: -x+1,-y,-z+2; #3: -x+1, y+1/2, -z+2; #4: x, -y+1/2, z; #5: x-1, y, z-1.

Table S7. The fitting parameters for fluorescence lifetimes at room temperature.

Compound	λ_{ex} (nm)	λ_{em} (nm)	τ_1 (ns)	A_1 (%)	τ_2 (ns)	A_2 (%)	<τ> (ns)	χ^2
CdCl-apim1	372	395	3.39	62.35	12.54	37.65	6.83	1.302
CdBr-apim1	372	395	1.83	52.12	6.62	47.88	4.12	1.065
CdCl-apim2	372	450	2.59	67.54	9.41	32.46	4.80	1.176
	450	500	3.00	63.13	8.25	36.87	4.93	1.216
CdBr-apim2	372	520	2.13	37.27	5.53	62.73	4.26	1.104
	405	480	2.36	59.09	6.17	40.91	3.92	1.058
	520	520	2.27	59.91	6.98	40.09	4.15	1.237

Table S8. The fitting parameters for phosphorescence lifetimes.

Compound	λ_{ex} (nm)	λ_{em} (nm)	T (°C)	τ_1 (ms)	A_1 (%)	τ_2 (ms)	A_2 (%)	<τ> (ms)	χ^2
CdCl-apim1	300	505	293	91.42	51.91	454.0	48.09	265.78	1.290
CdBr-apim1	330	515	293	4.57	49.95	14.5	50.05	9.52	1.134
CdCl-apim2	350	540	293	111.9	46.45	517.9	53.55	329.31	1.280
CdBr-apim2	345	540	293	14.97	50.90	65.23	49.10	39.65	1.231
			260	16.80	51.71	75.61	48.29	45.20	1.299
			220	20.89	53.18	93.59	46.82	54.93	1.218
			180	22.82	50.23	101.2	49.77	61.83	1.297
			140	23.92	51.36	101.7	48.64	64.38	1.299
			100	25.58	50.89	113.2	49.11	68.61	1.288
			80	28.08	51.31	123.5	48.69	74.54	1.227
	365	550	293	16.85	47.84	68.49	52.16	43.79	1.195
			260	17.36	48.55	72.98	51.45	45.98	1.279
			220	19.92	52.33	87.88	47.67	52.32	1.259
			180	22.21	52.25	96.68	47.75	57.77	1.273
			140	24.57	51.17	105.1	48.83	63.89	1.286
			100	24.51	52.49	110.4	47.51	65.32	1.278
			80	25.39	50.33	110.4	49.67	67.61	1.298
	395	575	293	19.80	48.40	72.58	51.60	47.03	1.211
			260	18.90	48.45	76.39	51.55	48.54	1.269
			220	23.66	49.37	92.70	50.63	58.61	1.255
			180	24.45	51.35	98.81	48.65	60.61	1.293
			140	24.18	51.64	103.8	48.36	62.68	1.245
			100	26.76	48.53	111.0	51.47	70.12	1.298
			80	27.05	51.52	115.9	48.48	70.12	1.257
	405	590	293	20.22	46.93	74.18	53.07	48.86	1.254